

A EUROPEAN FLIGHT DYNAMICS EXPERIMENT

Ph. Boland

ESA Earth Observation
Programme Office
Toulouse, France

ABSTRACT

The first flight dynamics experiment carried out with a European satellite is described. The purpose of the operation is to monitor the interaction between spin velocity and the torque produced by a thruster mounted on the main body of the satellite and parallel with the spin axis. The spacecraft of interest is GEOS-1, a spin stabilized satellite appended with two long wire booms. The objective of the paper is twofold. First, the historical background of the test is reminded and the context of a flight experiment is emphasized. This includes preflight analysis, preparation of flight operations and description of the experiment itself. Second, the dynamics phenomenon is analysed from both physical and mathematical aspects in the light of comparison between predictions and flight results.

Keywords : spacecraft, dynamics experiment, non-linear dynamics, flexibility.

1. INTRODUCTION

Only rarely do we have a chance to detect a potential anomaly in the behaviour of a spacecraft only a few days before a planned manoeuvre is executed and to thereby save the satellite. Such an opportunity was afforded by the GEOS-1 satellite in May 1979 when an orbit manoeuvre involving a long continuous burn of a thruster mounted parallel with the spin axis was to take place. Concern about possible dynamic interactions between external excitation and spin velocity, and resulting response of the cable booms of the vehicle, led to preflight simulations only to discover that the spacecraft should be destabilized and lost most likely few minutes after manoeuvre start.

This finding was soon confirmed by theoretical investigations so that the manoeuvre strategy was completely modified. This story would have probably been forgotten if an in-flight verification of predictions had not been realized successfully a few months later. This experiment, which stresses the importance of non-linear phenomena in flight dynamics, transformed the work of mathematical specialists from an intellectual approach to an interesting engineering experience.

2. BACKGROUND OF SUBJECT

2.1 History

GEOS-1 is a scientific magnetospheric-explorer

satellite launched on 20 April 1977 by the European Space Agency. This spacecraft had an eventful life which started with the acquisition of a rescue, elliptical 12 hour orbit, instead of the planned geostationary orbit, after the launcher had failed to inject the vehicle on the proper transfer trajectory. Some days later, when proceeding to the deployment of a pair of telescopic booms, one of them did not deploy fully which generated a peculiar and totally unexpected nutational motion of the spacecraft. All these troublesome events necessitated fast diagnosis and improvised corrective actions. During the mission, GEOS underwent many attitude and orbit manoeuvres generated by axial, radial and tangential thrusters, the most impressive being inversion manoeuvres operated around equinoxes to prevent excessive shadowing of solar arrays by the boom system. After supporting more than two years of extremely valuable scientific operations, surviving in an environment which was beyond the worst case design assumption, a final important orbit manoeuvre was planned in order to avoid too long eclipses and subsequent freezing of hydrazine.

GEOS is the first European satellite carrying flexible appendages. It is indeed composed of a main cylindrical body surrounded by several booms and antennas and two 20 m long wire booms stretched by centrifugal force (Figure 1). The nominal spin velocity is 10 rotations per minute. In this respect, extensive theoretical studies and simulations were performed to analyse its dynamic characteristics. Computer software were developed accordingly to predict and monitor its flight response to orbit and attitude manoeuvres.

Confidence grew in the dynamic stability of the satellite as the operations proceeded successfully until the time came to prepare the last orbit change. The manoeuvre consisted originally of a 45 minute continuous burn of an axial thruster mounted on the main body. However, despite previous happy experience, computer simulations of the complete operation were felt necessary by the flight dynamics support group, since there was some concern as to possible spin variations and resulting wild cable-boom oscillations. Inspecting computer results, not only did we find that our concern was relevant but we were surprised to see that complete despin and consecutive loss of the satellite was predicted within about five minutes (Ref. 1). A quick theoretical investigation based on previous studies (Ref. 2) was undertaken which confirmed the consistency of the results. With this level of understanding of the

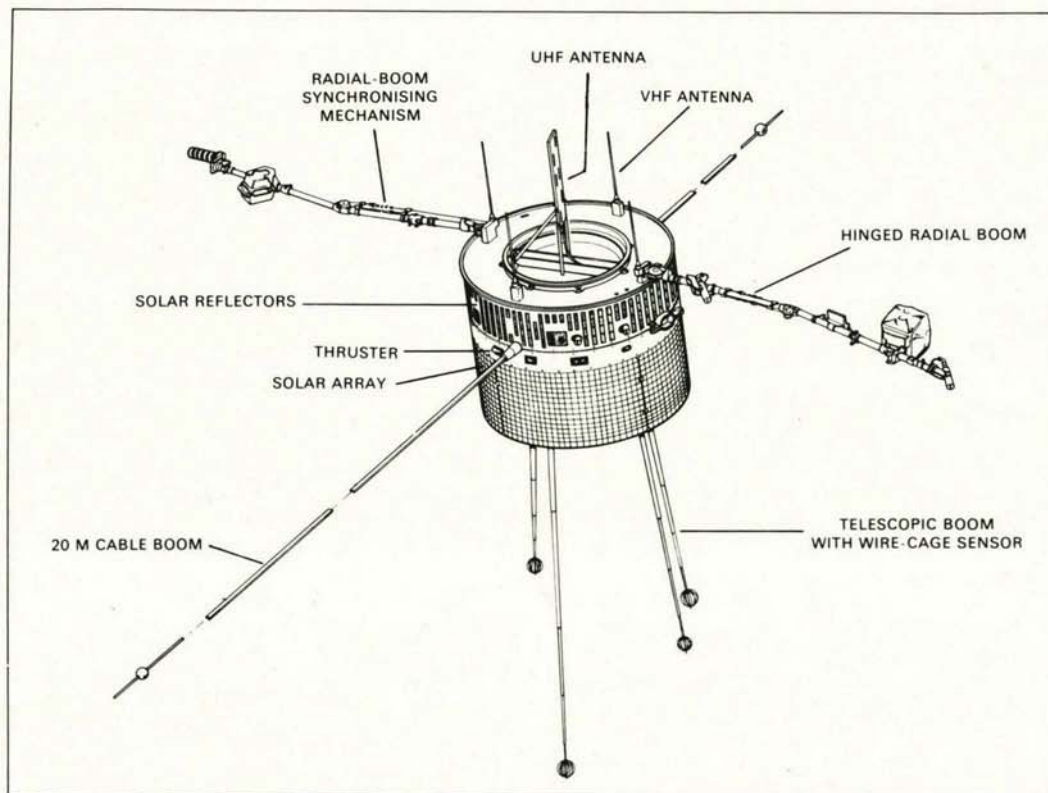


Figure 1. Lay out of GEOS Boom System

phenomenon it was decided to achieve the orbit manoeuvre using a radial thruster in pulsed mode instead of an axial thruster in continuous mode. This changed the manoeuvre duration from the original 45 minutes to 6 hours.

Considering the importance of this basic problem of flight dynamics, the group of dynamicists suggested later to proceed to in-flight verifications of theoretical predictions. This idea was supported by the ISPM project group since a similar situation could occur during an ISPM spacecraft mid-course correction manoeuvre if one of the axial thrusters were to fail. The operation was agreed by the Director of Scientific Programmes of the Agency and was implemented and conducted from the European Space Operation Center in Darmstadt on 27 and 28 September 1979.

2.2 Subject relevance

The GEOS-1 dynamic experiment has been presented in the first place in Ref. 3 with F. Janssens as co-author. F. Janssens devoted his efforts to present there a concise and comprehensive analytical formulation of the non linear effects whose importance was demonstrated with the flight experiment. However, the subject involves original operational aspects so that the Programme Committee found it an interesting theme to retain for presentation in the Symposium.

3. FLIGHT PLAN

A special flight plan (Ref. 4) was set up for the experiment since it is a time-critical operation which can only be reliably conducted in accordance with carefully prepared control procedures. Only the guidelines of Ref. 4 for this special type of

procedures are presented here.

3.1 General Description

Due to restricted ground station coverage the experiment must be split into two operation periods, which occur on consecutive days. The first period contains two spin-up manoeuvres and a first excitation manoeuvre (lower axial thruster in continuous mode) of 80 sec. The second period contains also a spin-up manoeuvre followed by a second excitation manoeuvre of 180 sec, nominally. The time separation between spin-up and excitation manoeuvres is two hours in order for the resulting cable boom oscillations to damp down.

The purpose of the spin-up segments is to achieve an initial spin rate of 11 RPM and to validate the spacecraft subsystems needed for the excitation phases (attitude and orbit control, attitude measurement and power supply systems). On the other hand, the first (short) excitation manoeuvre should demonstrate consistency between actual and predicted dynamic behaviour and prove correct functioning of the automatic on-board manoeuvre termination. Verification of satellite subsystems was particularly important since the satellite had been in hibernation state for several months and had transited through extremely long eclipses during that period.

Both excitation manoeuvres imply a continuous 7 Newton thrust in a direction parallel to the spacecraft spin axis. This thrust vector causes a spacecraft body fixed torque around an axis located in the equatorial plan of the satellite. Given the GEOS-1 thruster location and mass properties, this torque will cause increasing nutational motion and resulting deflections of long

radial booms and a decrease of the average spin rate. With the above indicated initial spin rate, simulations show that the spin rate will reach zero spin after 6.5 minutes. This is a condition that the spacecraft cannot survive without experiencing irrecoverable damage.

The durations chosen for the excitation manoeuvres ensure that these extreme conditions will not be met. In both cases, nutation and boom deflections should not exceed 15 deg. and the spin rate should remain above 8.5 RPM. These limits ensure proper functioning of the attitude measurement system (solar aspect angle and spin rate determination) and a good radio link with ground stations.

The optimal strategy for the experiment was set up on the basis of extensive computer simulation runs to cover a wide range of system parameters some of which were not accurately known (for instance, exact thrust level and quantity of residual fuel).

3.2 Purpose

The prime purpose of the flight tests is to establish the validity of theoretical predictions that led to changing the strategy of the last orbit manoeuvre planned for GEOS-1. This would also validate the mathematical model used for this flexible satellite when the system experiences large deformations. More generally, the importance of a little known non linear effect would be clearly demonstrated. Finally, as mentioned above, the ISPM project would be provided with a reliable input of this satellite under certain failure conditions which might necessitate some significant hardware changes.

3.3 Control technique

Both excitation manoeuvres will be conducted as mission-critical operations. For these, the decision making element is an enlarged flight control team consisting of experienced specialists for spacecraft operations and performance control, flight dynamics, ground facilities operations (stations, network, computers).

The spacecraft specialists will undertake real-time assessment of the on-board performance by referring to real time data displayed on alphanumeric, graphical and strip chart displays, and commanding of the spacecraft in manual mode for planned operations and contingency cases.

The flight dynamic specialists will undertake near real time assessment of the spacecraft attitude before and after the excitation manoeuvres and real time assessment of the dynamic behaviour of the spacecraft during and after the excitation manoeuvres.

3.4 Risks

The major danger for GEOS-1 would be exposure of the spacecraft to extremely violent dynamic motions which would result in destruction of the booms, damage to solar cells, loss of attitude and controllability and problems with the power supply. Such a situation could arise if the excitation manoeuvre were not terminated within 6 minutes after commencement or if the build-up of dynamic instability were actually faster than predicted.

Flight control procedures were defined so that

both cases could be kept under control in order to minimize the risks inherent in excitation manoeuvres.

4. EXPERIMENT PREPARATION

4.1 System modelling

Despite the many flexible booms and antennas that surround the main body of the GEOS satellite (Figure 1), the overall dynamic response of the system can be simulated satisfactorily by a simple model including one rigid body and two hinged bars to represent the 20 m cable booms, the remaining appendages being considered as rigid. The bars are assigned the same mass and inertia characteristics as the corresponding flexible elements. Detailed analysis shows in fact that the deformation modes for which the cables depart substantially from a straight line can be ignored. The connections between the central body and the cable booms are represented by two-degree-of-freedom joints, so that the resulting relative motions can be broken down into oscillations in one plane perpendicular to the spin axis (equatorial plane), and another containing that axis (meridian plane). No damping is represented, although GEOS is equipped with a particularly effective nutation damper and root dampers

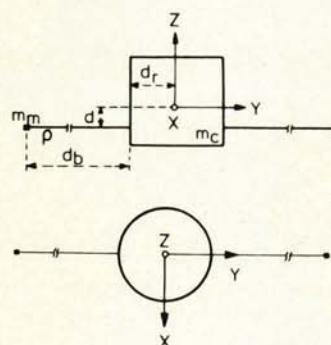


Figure 2. Satellite Mathematical Model

Table 1. Input data in reference frame (Fig. 2)

| | |
|--|-----------------------------------|
| Main body | |
| Mass (kg) | : 273.68 (including 4 kg of fuel) |
| Height of CG above separation plane (m) | : 0.502 |
| Inertias along X, Y, Z (kgm ²) | : 78.37, 163.51, 170.98 |
| Cable booms | |
| Root location (m) | : (0. \pm 1.101, -0.1797) |
| Specific mass (kg m) | : 0.0224 |
| Length (m) | : 19.75 |
| Tip mass (kg) | : 0.1072 |
| Lower axial thruster | |
| Location (m) | : (0.555, 0.466, -0.394) |
| Direction | : (0, 0, 1) |
| Level (N) | : 7 |
| Mode | : continuous |
| Inclined accelerometer | |
| Location (m) | : (-0.6925, 0, 0.2763) |
| Sensitive direction | : (0, 0.7071, -0.7071) |
| Vertical accelerometer | |
| Location (m) | : (0, -0.6925, 0.3731) |
| Sensitive direction | : (0, 0, 1) |



Figure 3. Magnitude of Angular Momentum v.s time

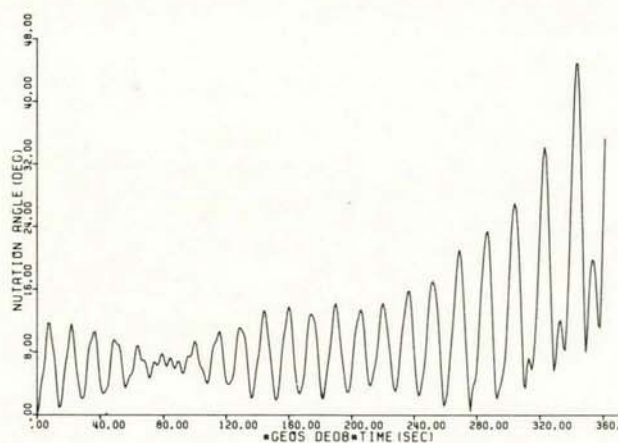


Figure 5. Nutation Angle v.s time

for the cable booms. This omission has no major consequences as far as the dynamical phenomenon of interest is concerned, namely the spin variations associated with the action of an axial external force on the satellite.

The pre-flight simulation of the planned test manoeuvre was made with a generic, discrete-coordinate simulation program. This digital computer program has the capacity to simulate the large-angle motion (nonlinear equations) response of interconnected rigid-body systems to external forces, with possible constraints for the interbody connections. The program is currently being used for preliminary studies of the attitude dynamics and appendage-deployment phases of spacecraft with flexible appendages. Such investigations may have a considerable impact on manoeuvre strategies (the subject of this paper being a dramatic example), mechanical design and control-system definition (Ref. 5).

4.2 Pre-flight simulations

We shall now analyse qualitatively the dynamic behaviour of GEOS as predicted by computer simulation when the lower axial thruster is operated in continuous mode. The basis of the mathematical model is shown in Figure 2. The satellite's mass and configuration at the time of the dynamic experiment are summarised in Table 1, the frame of reference being

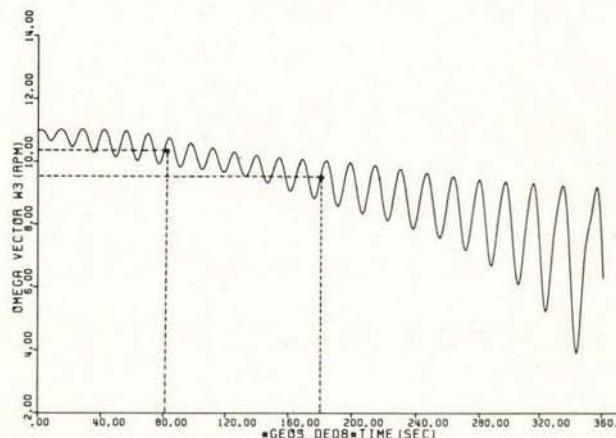


Figure 4. Axial component of Spin Vector v.s time

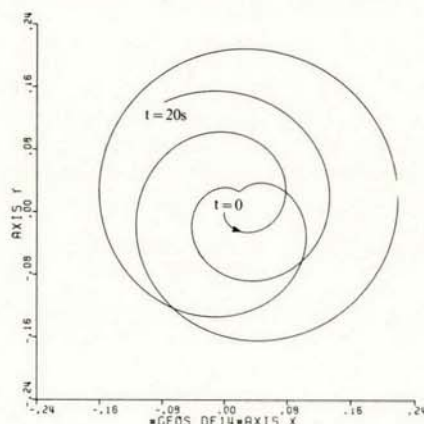


Figure 6. Inertial Motion of Spin Axis

centred on the main body's centre of mass, with the orientation indicated in Figure 2.

Let us concentrate first on the variations in the system's total angular momentum. The axial force fixed in the main body generates a spinning torque which is perpendicular to the angular momentum when the excitation starts. As one may anticipate intuitively, a unit vector aligned with the angular-momentum vector will describe a cone in inertial space, at spin frequency. In the present case the corresponding cone half-angle remains smaller than 1° . Of more interest is the time history of the magnitude of the angular momentum, which undergoes a systematic deviation from its nominal value, as illustrated in Figure 3. If the action of the external torque is stopped at some particular instant, the angular momentum will remain constant and the satellite will reacquire its equilibrium configuration after the system oscillations have damped out. The resulting spin rate is then easily calculated as the ratio between the magnitude of the angular momentum and the spin inertia of the system. From this we can conclude that the satellite's instantaneous mean spin rate must vary in much the same way; this is confirmed in Figure 4, where the third component of the omega vector is plotted as a function of time.

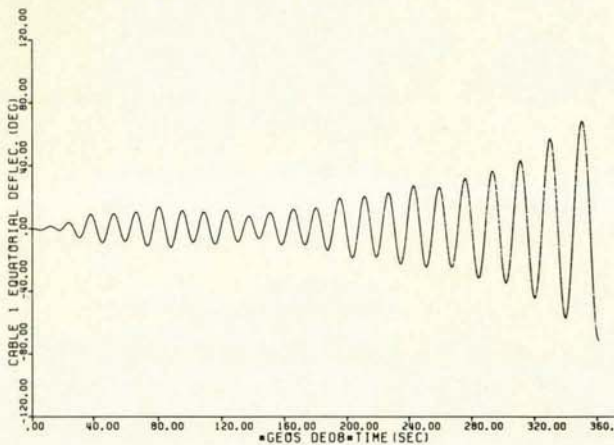


Figure 7. Equatorial Deflections of Cable v.s time

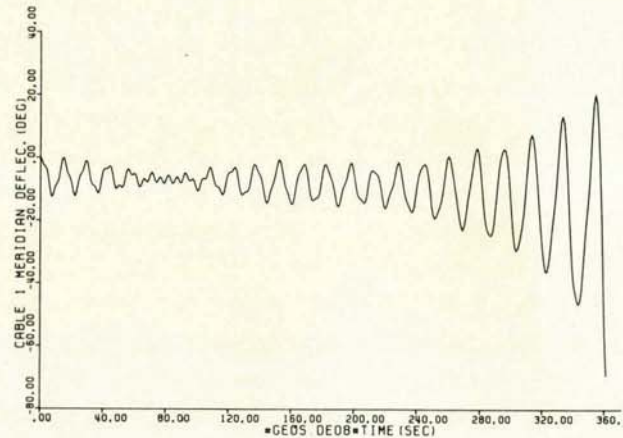


Figure 8. Meridian Deflections of Cable v.s time

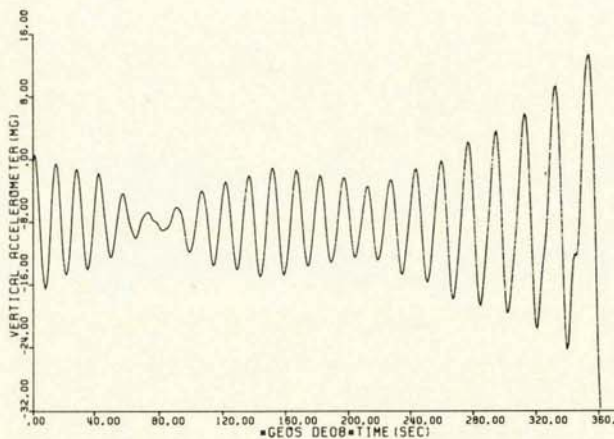


Figure 9. Vertical Accelerometer Signal v.s time

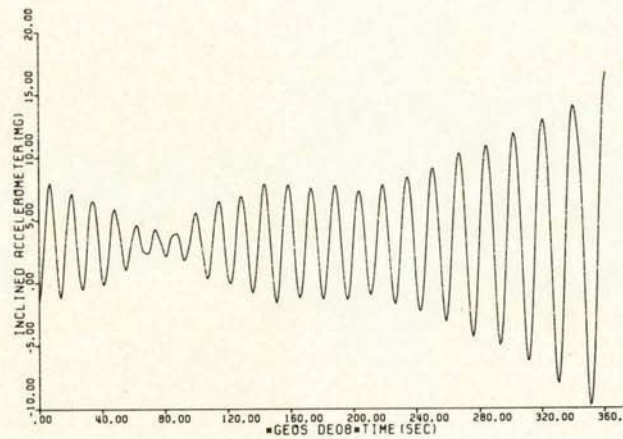


Figure 10. Inclined Accelerometer Signal v.s time

It is worth noting that such dynamic behaviour is not predictable on the basis of linearised equations of motion. Linear analysis shows, on the contrary, that the spin rate should be constant during such excitation. The despin phenomenon must, therefore, be attributed to nonlinear effects. This is deduced on an analytical basis in the next section. A sound understanding of the problem can, however, be gained by considering the spacecraft motions, as explained below.

When the continuous axial force is applied, the body-fixed Z-axis (Figure 2) begins to wander about the angular momentum vector. The nutation angle (measured between these two directions) is plotted against time in Figure 5. The resulting oscillations are at the nutation frequency for this type of excitation, whereas twice this frequency is always associated with the nutation-angle variation when the motion is force-free. The nutation frequency is a characteristic frequency of the system and is identified from modal-analysis considerations.

The motion of the centre body in inertial space can be visualised by examining the trace of the body-fixed Z-axis on a plane fixed in inertial space. This is shown in Figure 6, where the plane of reference is perpendicular to the body Z-axis when the manoeuvre is initiated.

From the comments above it is clear that the body-fixed torque vector corresponding to the applied force and the angular-momentum vector do not remain perpendicular to each other, due to nutation. The work produced by the continuous torque therefore varies periodically at the nutation frequency. From this it can be conceived that the mean value of this function over a nutation period does not necessarily average to zero, but rather depends on geometric characteristics of the system. The conditions that govern the variations in the angular momentum are established in the final section of this paper.

It should be clear from the preceding arguments that the spin variations are forced at nutation frequency (Figure 4). The cable booms are in turn forced into antisymmetric oscillations in the equatorial plane at the same frequency. The relative angular displacements of one cable in the equatorial plane with respect to the centre body is shown in Figure 7. As outlined previously, this is a nonlinear response to the type of perturbation under consideration, since the eigenfrequency of the system which characterises this type of cable boom motion is basically different for this length of cables.

Turning our attention now the oscillations of the cables in the meridian plane, we can see by simple examination that the traces of Figures 5 and 8 are similar but of opposite sign. This is typical of the so-called nutation mode of this mechanical system, which can be identified from linear equations. The cables experience antisymmetric displacements for this mode, which is always coupled with a higher frequency but otherwise similar mode, the so-called meridian antisymmetric mode. This high-frequency vibration is clearly present in Figures 5 and 8.

Another characteristic of Figures 4, 5, 7 and 8 is the modulation in amplitude of the corresponding signals. The periods of modulation can be obtained by introducing the spin-rate variations at nutation frequency into the linearised equations of motion. This changes the linear equations with constant coefficients into linear equations with periodic coefficients. The observed modulations can then be explained in terms of parametric excitations.

To summarise, the general dynamic behaviour of GEOS under continuous axial thrusting conditions is governed essentially by the nonlinear part of the equations of motion, although some system modes typical of linear response are also present. The long-term effect of the resulting torque is a despinning of the spacecraft and a consecutive build-up of nutational motion, as illustrated in Figure 5, the cable booms making wild oscillations at the same time (Figures 7 & 8). It should be noted that the cables themselves could become slack long before that moment.

4.3 Monitoring of the manoeuvre

The dynamic behaviour of the GEOS satellite is monitored mainly by the pair of on-board accelerometers, the exact locations of which are given in Table 1, their sensing directions being parallel (vertical accelerometer) and inclined by 45° (inclined accelerometer) to the body-fixed Z-axis. The corresponding telemetry output is plotted in real time on strip-chart recorders in the Control Room at (ESOC). This provides immediate insight into spacecraft behaviour and, at the same time, a valuable base for real-time decision making during a manoeuvre. The computer-simulated accelerometer traces corresponding to Figures 3-8 are reproduced in Figures 9 and 10.

Spin rate is measured via the satellite's optical sensor system, which is designed to provide only one type of measurement every 45 s. In this respect it was not possible to assess the mean spin rate until well after the manoeuvre had been completed; neither was it possible to monitor the constantly changing attitude of the spacecraft during the manoeuvre with the set of solar and earth sensors.

5. COMPARISON OF FLIGHT AND TELEMETRY DATA

Table 2 compares the spin variations obtained by computer simulation and those measured on-board the satellite; the excellent agreement is readily apparent. The corresponding points are indicated in Figure 4.

Telemetry data were used to produce the plots of Figures 11 and 12, corresponding to the first and second manoeuvres. A direct comparison is shown with the computer-simulated outputs, which had been scaled to the format of the strip-chart records. The accelerations are measured in milli-g's as a

function of time in seconds. The saturation level at ± 12.5 mg has been included in the predictions.

The acceleration at any point in the main body depends on all of the system parameters. Any deficiency in the system modelling may therefore affect the resemblance between the simulated and actual time histories of these accelerations. Nevertheless, Figures 11 and 12 show good agreement between predictions and real-time telemetry data for the on-board accelerometer outputs.

The differences in magnitude which can be observed are attributed to damping, which was not incorporated in the mathematical modelling. In this respect, the amplitude modulation of these signals is much less pronounced for the actual data, although it is still quite visible. The predictions show a shift in the phase of the accelerometer signals as a result of the narrowing associated with the amplitude modulation. This phenomenon is not reproduced in the actual accelerometer outputs. As a direct consequence, the amplitudes of accelerations corresponding to the consecutive free motions are different. This is particularly apparent for the second manoeuvre.

Table 2

| Manoeuvre | First | Second |
|----------------------|-----------|-----------|
| Duration | 82 sec. | 181 sec. |
| Initial spin | 10.97 RPM | 11.00 RPM |
| Final spin predicted | 10.36 RPM | 9.50 RPM |
| Final spin measured | 10.36 RPM | 9.53 RPM |

6. MATHEMATICAL FORMULATION

6.1 Rigid body

Since the Symposium is devoted to operational aspects, only a short mathematical presentation of the problem will be made here. It will however enlighten the reader on the key feature that made the experiment possible. As mentioned in section 2, a more comprehensive treatment is available in Ref. 3.

We shall first concentrate on a rigid body spinning uniformly around its axis of maximum inertia and acted on by an axial thruster set in continuous mode (step function). Since the thruster is not located on the spin axis, a body-fixed constant equatorial torque is applied to the rigid body. We consider the mass variation due to fuel consumption as negligible. This is a special case of a similar problem with the only difference that the external force consists of a series of identical pulses (Ref. 2).

The corresponding Euler equations are :

$$\begin{aligned}
 A \dot{\omega}_1 + (C - B) \omega_2 \omega_3 &= t_1 \\
 B \dot{\omega}_2 + (A - C) \omega_3 \omega_1 &= t_2 \\
 C \dot{\omega}_3 + (B - A) \omega_1 \omega_2 &= 0 \\
 A < B < C
 \end{aligned}
 \tag{1}$$

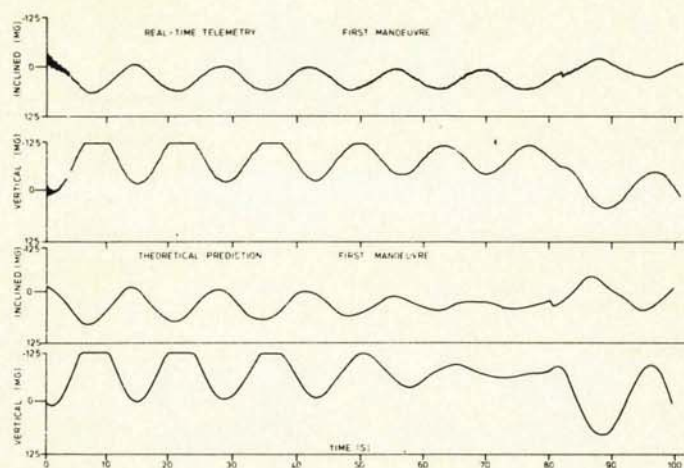


Figure 11. Accelerometer telemetry/predictions
First manoeuvre

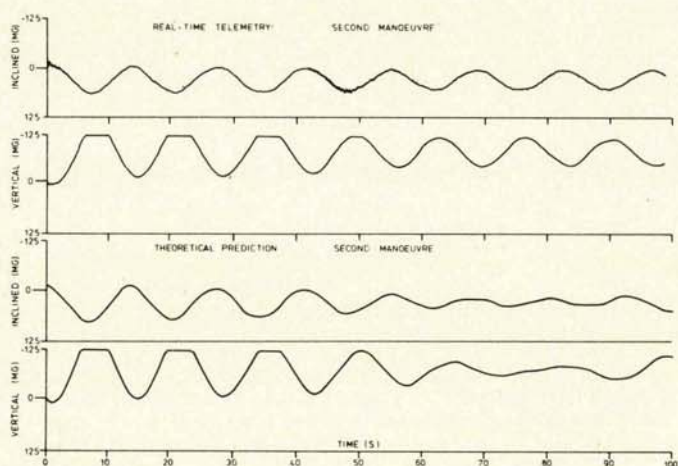


Figure 12 a) Accelerometer telemetry/predictions
Second manoeuvre

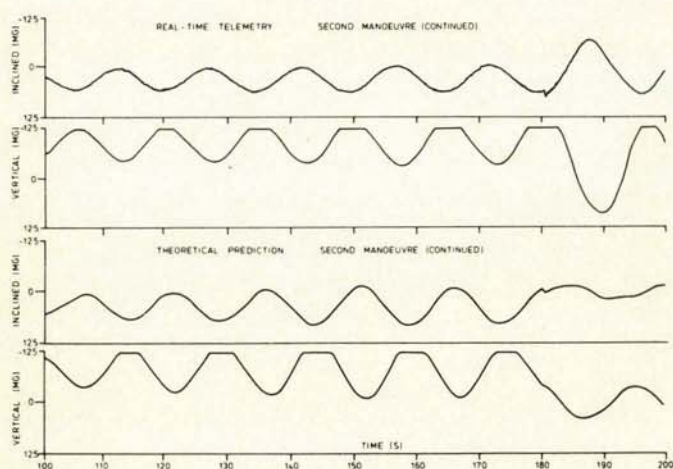


Figure 12 b) Accelerometer Telemetry/predictions
Second manoeuvre (continued)

with initial conditions

$$\omega_1(0) = \omega_2(0) = 0 \quad \omega_3(0) = \omega_0 \quad (2)$$

If we linearize the first two of Eqs. 1 around the initial conditions given in Eq. 2, assuming small perturbations of ω_2 and ω_3 , we obtain the corresponding solutions :

$$\omega_1(t) = \frac{t_1}{A\omega_0 N} \sin \omega_0 N t - \frac{t_2}{(C-A)\omega_0} (1 - \cos \omega_0 N t) \quad (3)$$

$$\omega_2(t) = \frac{t_2}{B\omega_0 N} \sin \omega_0 N t + \frac{t_1}{(C-B)\omega_0} (1 - \cos \omega_0 N t)$$

$$\text{with } N^2 = \frac{(C-A)(C-B)}{AB}$$

$\omega_0 N$ being the nutation frequency. From Eqs. 3 we can see that the mean value Ω_1 of ω_1 and Ω_2 of ω_2 over one nutation period are given by the constants in Eqs. 3 whereas corresponding mean values for $\dot{\omega}_1$ and $\dot{\omega}_2$ are zero.

Returning now to the consideration of Eq. 1 with the following assumption :

- oscillations of ω_1 and ω_2 remain small
- ω_3 experiences small oscillations with a mean value Ω_3 quasi-constant over one nutation period

and if we integrate the first two of Eqs. 1 over any nutation period for which the above conditions are satisfied, we obtain :

$$\Omega_1 = \frac{-t_2}{(C-A)\Omega_3} \quad (4)$$

$$\Omega_2 = \frac{t_1}{(C-B)\Omega_3}$$

where the mean values of ω_1 and ω_2 depend explicitly on the instantaneous (but slowly varying) mean value Ω_3 of ω_3 . The same procedure applied to the third of Eqs. 1 provides, with the combination of Eqs. 4 :

$$\Omega_3 = \frac{t_1 t_2}{\Omega_3^2} \frac{B-A}{C(C-A)(C-B)} \quad (5)$$

where Ω_3 is the average change in ω_3 . Eq. 5 is easily integrated by separations of variables, so that :

$$\Omega_3(t) = \omega_0 \left(1 + \frac{t - t_0}{\tau} \right)^3 \quad (6)$$

with

$$\tau = \frac{3}{\omega_0} \frac{C(C-A)(C-B)}{3t_1 t_2 (B-A)} \quad (7)$$

The following interesting conclusions can be deduced immediately from Eqs. 5 and 6 :

- The initial spin rate remains constant in average if the body is symmetric or if the thruster location coincides with a principal axis.
- Spin-up occurs if $t_1 t_2 > 0$, that is if the thruster is located in the second or fourth quadrant.
- Spin-down occurs if the thruster is located in the first (GEOS case) or third quadrant.
- The spin effect is independent of the direction of the axial force (up or down).
- A spin-down is quasi-linear as long as the average spin is not close to zero. When the spin approaches zero, the spin down is very sharp. This phenomenon is not well reflected by Eq. 6 since the basic assumptions are no longer valid (Ω_3 cannot be taken as constant during one nutation period).
- A spin up is slower and slower as the average spin increases.

6.2 The GEOS case

Since GEOS is appended with two wire booms, deformation equations must be considered for the boom motions that prevail during the excitation manoeuvre together with the Euler equations for the total system. An equivalent modelling of the cable booms consisting of two pendulums is presented in Ref. 6 which is the basis for the developments of Ref. 3 leading to an equation identical to Eq. 6 to describe the time history of the average spin velocity under continuous axial thrusting, except that Eq. 7 becomes now :

$$\tau = \frac{\omega_0^3}{3t_1 t_2} \frac{C'(C-A)(C-B')}{B-A} \quad (8)$$

with $B' = B - 2 m_T$ $a(a+1)$

$C' = C + 2 m_T (a+1)^2$

where

a = distance of pendulum attachment point from spin axis

l = equivalent length of pendulums

m_T = equivalent tip mass

A, B, C = central body inertias

using the input data of Table 1 and, from Ref. 3, $l = 13.412$ m, $m_T = 0.56$ Kg so that $B' = 145.631$ Kg m^2 and $C' = 406.86$ Kg m^2 , predictions from Eqs. 6 & 8 for the final spin rates obtained during the excitation manoeuvres are compared to real data in table 3.

Table 3

| Manoeuvre | First | Second |
|----------------------|-----------|----------|
| Final spin measured | 10.36 RPM | 9.53 RPM |
| Final spin predicted | 10.25 RPM | 9.27 RPM |

7. CONCLUSION

Whatever the level of confidence we have acquired in a satellite dynamic behaviour, all new type of manoeuvre must be analysed carefully from complete modelling. We are indeed generally tempted to resort to oversimplified models or equations without having the insurance that the approximations we make are correct. In this respect, if linearized equations of motion may provide a sound insight into the dynamic behaviour of a satellite, we must realize that they reflect only a small part of reality. A more realistic approach consists in devising simplified theories to explain phenomena that came into light from a more general approach.

The GEOS dynamic experiments demonstrated the evidence of a little known coupling between spin velocity and forces parallel with the spin axis of spinning satellites. Depending on vehicle mass properties and general configuration, this effect may have dramatic consequences, reducing the spin velocity rapidly, and thereby destabilizing the spacecraft.

8. ACKNOWLEDGMENT

The GEOS-1 dynamics experiment was organized within the framework of the Mathematical Analysis Division of the European Space Technology Center in collaboration with F. Janssens and J. Schniewind. The operations were conducted by W. Wimmer, GEOS spacecraft operation manager.

9. REFERENCES

1. ESA EWP 1194 1979, *Theoretical predictions for GEOS-1 Dynamic experiment*, by Boland Ph. & Janssens F.
2. ESA EWP 1063 1978, *Spin rate variations of an asymmetric spinning rigid body submitted to axial forces*, by Boland Ph.
3. Boland Ph. & Janssens F. 1979, The GEOS-1 dynamic experiment, *ESA Journal* Vol. 3, 265-280.
4. ESOC GEOS FOP 1979, *GEOS-1 flight operation plan for the dynamic experiment*, by Wimmer W, Heger D & Leroux R.
5. ESA STM-216 1980, *User's guide for a computer simulation program for multi-rigid body systems*, by Boland Ph.
6. Janssens F. 1976, Dynamics of spinning satellites modelled as a rigid central body and spherical pendula as appendages. *Proc of Symposium on the dynamics and control of non-rigid satellites*, Frascati 24-26 May 1976, ESA SP 117, 39-40.